Stroboscopic Effect between Electronic and Nuclear Motion in Highly Excited Molecular Rydberg States

P. Labastie, M. C. Bordas, B. Tribollet, and M. Broyer
Laboratorie de Spectrométrie Ionique et Moléculaire, Université Lyon I, F-69622 Villeurbanne Cédex, France

(Received 14 February 1984)

The Na_2 Rydberg states have been observed for $15 \leq n \leq 90$ and $4 \leq J \leq 45$. The evolution of the spectra is studied as a function of the relative values of ω_{el}, the electronic rotational frequency, and ω_N, the nuclear rotational frequency. The molecular eigenfunction is found to be pure Hund's case *a* when $k\omega_{el} = 2\omega_N$ (k being an integer). This may be explained in terms of stroboscopic effects arising from the movement of the Rydberg electron relative to the ionic core.

PACS numbers: 33.80.Eh, 33.10.−n

In highly excited molecular Rydberg states, the rotational frequency ω_{el} of the Rydberg electron in its orbital motion can become smaller than the rotational frequency ω_N of the nuclei. Under these conditions, the Born-Oppenheimer approximation is no longer valid and the electron angular momentum $\vec{l}$ tends to be decoupled from the internuclear axis.

The interpretation of these effects was rather involved,[1] until the experimental work of Herzberg and Jungen[2] on H_2 whose interpretation by quantum-defect theory was due to Fano.[3] However, in their experiment they observed only Rydberg levels with $n \leq 40$ and $J = 0,1,2$.

Recently optical-optical double resonance[4–8] has proved to be a powerful technique to study molecular Rydberg states. Using this method we have observed Na_2 molecular Rydberg states for $15 \leq n \leq 90$ and $4 \leq J \leq 45$. These new results enable us to study in detail the molecular spectrum when $\omega_{el} \simeq \omega_N$ or $\omega_{el} \ll \omega_N$.

In the intermediate region $\omega_{el} \simeq \omega_N$, where the spectra should be complicated, some simplification occurs when $k\omega_{el} = 2\omega_N$ (k an integer), because of stroboscopic effects between the two frequencies.

The experimental setup consists of a supersonic sodium beam crossed at right angles by two superimposed tunable dye lasers pumped by the same pulsed yttrium aluminum garnet laser.[9] The first laser selects a well-defined rovibrational level (v',J') of the Na_2 $A\,{}^1\Sigma_u^+$ state. The second laser excites the (v,J) levels in the *nd* complex. Beyond the ionization limit, these states with $v \geq 1$ are autoionizing by vibrational coupling. The electrons are then collected by a pulsed electric field which lags behind the laser pulses by ~ 30 ns, and they are then detected by means of an electron multiplier.

At low n values $\omega_{el} >> \omega_N$, which is the usual condition for validity of the Born-Oppenheimer approximation. The projection Λ of the electronic angular momentum $\vec{l}$ onto the internuclear axis is a good quantum number. The lines have the usual molecular structure, P, Q, R. However, Λ doubling occurs and the P, Q, R lines are not equidistant. We observe $nd\,{}^1\Sigma_g$, $nd\,{}^1\Pi_g$, $nd\,{}^1\Delta_g$ series. The occurrence of $\Sigma \rightarrow \Delta$ transitions is explained by the mixing of wave functions, due to Λ doubling.[9]

As n increases, rotational perturbations become important, and the regular structure of the spectrum is lost. For the interpretation of these spectra we have used the multichannel quantum-defect theory introduced by Seaton,[10] and applied to molecular Rydberg states by Fano.[3] The theoretical aspects are described elsewhere.[11] Let us summarize here the relevant equations of the problem.

At given J and $l = 2$, we have five ionization channels: $N^+ = J-2, \ldots, J+2$ (where N^+ is the angular momentum of the ion). These five channels split into two for levels of minus symmetry ($N^+ = J-1, J+1$) and three for levels of plus symmetry ($N^+ = J-2, J, J+2$). The eigenchannels are those of Hund's case *a*, i.e., $nd\,{}^1\Pi_g^-$, $nd\Delta_g^-$ for the minus series and $nd\,{}^1\Sigma_g^+$, $nd\,{}^1\Pi_g^+$, $nd\,{}^1\Delta_g^+$ for the plus series. The eigen quantum defects have been found in Ref. 9 to be: $\mu_{d\Sigma} = 0.21$, $\mu_{d\Pi} = -0.04$, and $\mu_{d\Delta} = 0.43$. The transformation matrix from ionization to eigenchannels is the Hund's case-*d* to Hund's case-*a* transformation matrix $U^{Jl}_{\Lambda N^+}$ which is known by standard Racah algebra. We define the effective quantum numbers ν_{N^+} as

$$E = T_\infty(v) + BN^+(N^+ + 1) - R/(\nu_{N^+})^2, \quad (1)$$

where E is the energy of the state of interest, B the rotational constant of the molecular ion, and R the

Rydberg constant. This equation gives $i-1$ relations between the ν_{N^+}'s, where i is the number of channnels.

If we write the wave function in the case-a basis

$$|\psi\rangle = \sum_\Lambda A_\Lambda |l\Lambda J\rangle, \tag{2}$$

the multichannel quantum-defect theory gives the following set of equations[12]:

$$\sum_\Lambda A_\Lambda U^{Jl}_{\Lambda N^+} \sin\pi(\nu_{N^+}+\mu_\Lambda) = 0 \tag{3}$$

for each N^+. This system has nonzero solutions when

$$\det[U^{Jl}_{\Lambda N^+} \sin\pi(\nu_{N^+}+\mu_\Lambda)] = 0. \tag{4}$$

Equation (4) together with relation (1) determines the discrete energy levels. The A_Λ's are then found by resolution of Eq. (3). The results of multichannel quantum-defect theory analysis permit a precise reproduction of experimental spectra to be calculated,[11] as illustrated by Figs. 1, 2, and 3. We emphasize here some peculiar features of these spectra.

As pointed out by Lu,[13] when all the ν_{N^+}'s are equal modulo 1, Eqs. (4) and (3) have a simple solution

$$\nu_{N_1^+} = n-\mu_{\Lambda_0} \equiv \nu_{N_2^+} \equiv \ldots (\mathrm{mod}\,1), \qquad A_\Lambda = \delta_{\Lambda\Lambda_0}. \tag{5}$$

The eigenfunctions are then pure Hund's case a functions.

Now, let us consider the case of series of minus symmetry (the same analysis may be pursued for plus symmetry). Equation (1) gives

$$\nu_{J-1} = \nu_{J+1}[1-(4B/R)(J+\tfrac{1}{2})\nu^2_{J+1}]^{-1/2}. \tag{6}$$

While

$$(4B/R)(J+\tfrac{1}{2})\nu^2_{J+1} \ll 1, \tag{7}$$

the derivative $d\nu_{J-1}/d\nu_{J+1} \simeq 1$, so that the difference $\nu_{J-1}-\nu_{J+1}$ is a constant for variations of ν_{J+1} over a few integer values. However, even when (7) is fulfilled, this difference may be an integer value, since

$$\nu_{J-1}-\nu_{J+1} \simeq (4B/R)(J+\tfrac{1}{2})\nu^3_{J+1}. \tag{8}$$

This fact is important: The difference $\nu_{J-1}-\nu_{J+1}$ may be an integer and keep this value during a few levels, so that a whole region of the spectrum satisfies Eq. (5). In this region, the spectra are strongly simplified, because $^1\Delta$ lines are forbidden, the $^1\Pi$ lines are much more intense than the $^1\Sigma$ ones, and the P, Q, R lines lie at the same energy. This is illustrated in Fig. 1. Indeed, a "periodic return" of the system to Hund's case a occurs when $\nu_{J-1}-\nu_{J+1}$ is an integer.

The classical interpretation of this effect is illuminating. If ω_{el} and ω_N are the classical frequencies of the electronic and nuclear motion, respectively, we have

$$\hbar\omega_{el} \simeq 2R/3, \quad \hbar\omega_N \simeq 2B(J+\tfrac{1}{2}). \tag{9}$$

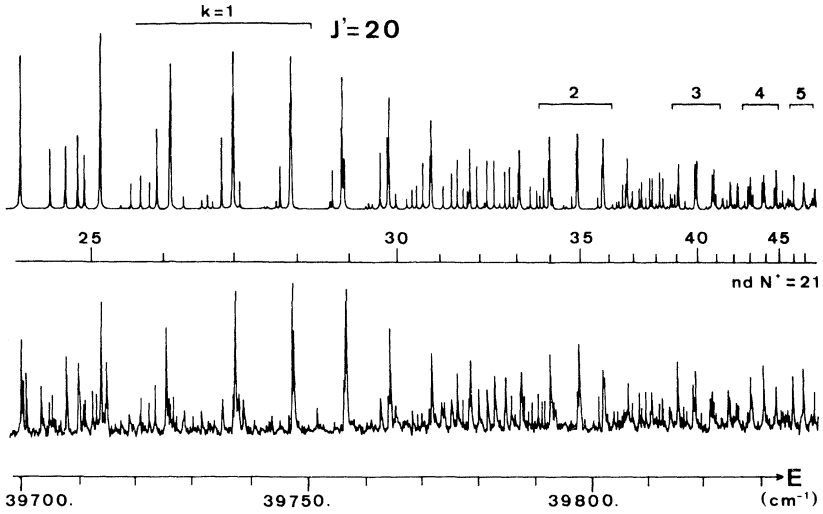

FIG. 1. Theoretical (upper) and experimental (lower) spectra are shown for the $A\,^1\Sigma_u^+$, $v'=3$, $J'=20$ intermediate level. Simplifications corresponding to $k=1,2,3,4,5$ are clearly observed. The levels of the series $nd\,N^+=J+1$ are also given.

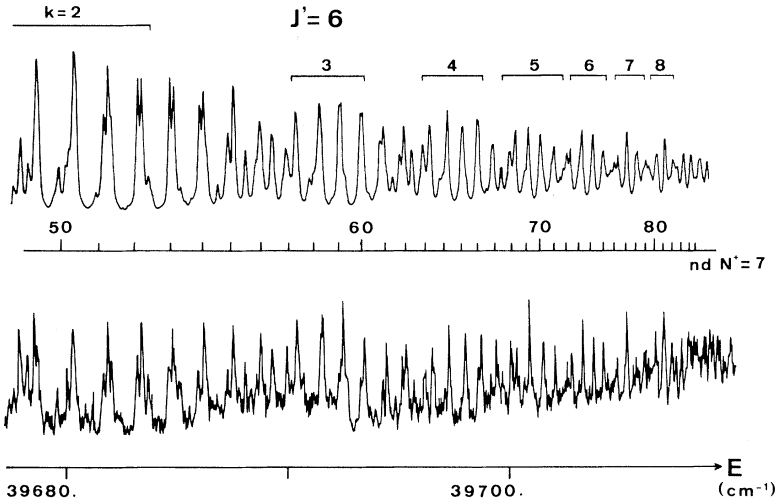

FIG. 2. Theoretical (upper) and experimental (lower) spectra are shown for the $A\,^1\Sigma_u^+$, $v'=2$, $J'=6$ intermediate level. In the region $50 \leq n \leq 90$, stroboscopic effects always occur corresponding to $k=2,3,4,5,6,7,8$.

In fact the electron "sees" the detailed structure of the core (in particular the internuclear axis) only when it passes through it. Hence, it "lights" the core like a stroboscope at frequency ω_{el}. The internuclear axis seems at rest when it makes an integer number of half turns during an electron period, i.e., when $2\omega_N = k\omega_{el}$. This is precisely the condition $\nu_{J-1} - \nu_{J+1} = k$. Since the axis seems at rest, the projection Λ of $\vec{l}$ onto this axis is a good quantum number, and the coupling is Hund's case *a*.

The observation of these stroboscopic effects is strongly dependent on the value of $\hbar\omega_N$, i.e., of $B(J+\frac{1}{2})$: It must be possible to satisfy simultaneously (7) and $2\omega_N/\omega_{el} = k$, which imposes

$$[R/B(2J)k]^{1/3} >> 1. \tag{10}$$

Condition (10) is valid at low BJ values, and was not fulfilled in H_2,[2] even at $J=1$, so that these stroboscopic effects have never previously been observed.

Stroboscopic effects are observed when $k\omega_{el} = 2\omega_N$ but k is not allowed to be too high, since the condition (10) would no longer hold. In fact, a new aspect of the spectra appears in the region of few $h\omega_N$ below the ionization limit. The main effects

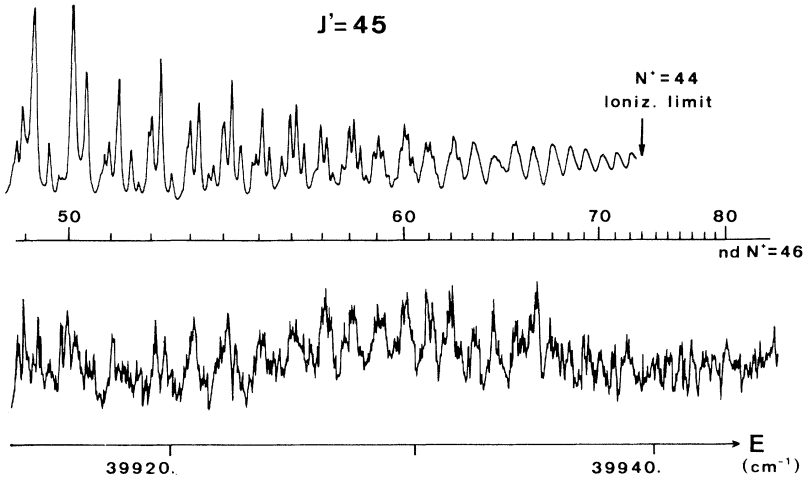

FIG. 3. Theoretical (upper) and experimental (lower) spectra are shown for the $A\,^1\Sigma_u^+$, $v'=2$, and $J'=45$ intermediate state. In the region $50 < n < 90$ quasi-Fano profiles are observed, but no stroboscopic effects. The signal-to-noise ratio is too low to observe experimentally the lines of the $nd\,N^+ = J-1$ series inside the quasi-Fano profiles.

in this region can be explained by the interaction of two Rydberg series: a very dense series of levels converging towards the $nd\ N^+ = J' - 1$ limit which forms a quasicontinuum, and the levels of the other $nd\ N^+ = J' + 1$ series. Indeed these two series are the only ones allowed by the selection rule $\Delta N^+ = 0$, i.e., $N^+ = J' \pm 1$. Hence, each line of the second series is a quasi-Fano profile filled with the lines of the other one.

This Fano profile region is not obtained on our experimental spectra if J' is too low. Figure 2 shows a $J' = 6$ spectrum in the range $50 < n < 90$. Many stroboscopic oscillations are seen, but no Fano profiles. On the other hand, Fig. 3 shows a $J' = 45$ spectrum in the same range. Here quasi-Fano profiles appear as broad lines, since the individual lines of the $nd\ N^+ = J' - 1$ series are not resolved. Note that the experimental spectrum extends also beyond the $N^+ = J' - 1$ ionization limit, where quasi-Fano profiles become true ones.

Laboratoire de Spectrométrie Ionique et Moléculaire is a laboratoire associé au Centre National de la Recherche Scientifique.

[1]Y. N. Chiu, J. Chem. Phys. **41**, 3235 (1964); R. S. Mulliken, J. Am. Chem. Soc. **86**, 3183 (1964), and **88**, 1849 (1966), and **91**, 4615 (1969).

[2]G. Herzberg and Ch. Jungen, J. Mol. Spectrosc. **41**, 425 (1972).

[3]U. Fano, Phys. Rev. A **2**, 353 (1970).

[4]N. W. Carlson, A. J. Taylor, and A. L. Schawlow, Phys. Rev. Lett. **45**, 18 (1980).

[5]S. Leutwyler, A. Herrmann, L. Wöste, and E. Schumacher, Chem. Phys. **48**, 253 (1980).

[6]S. Martin, J. Chevaleyre, S. Valignat, J. P. Perrot, M. Broyer, B. Cabaud, and A. Hoareau, Chem. Phys. Lett. **87**, 235 (1982).

[7]M. Broyer, J. Chevaleyre, G. Delacretaz, S. Martin, and L. Wöste, Chem. Phys. Lett. **99**, 206 (1983).

[8]M. Seaver, W. A. Chupka, S. D. Colson, and D. Gauyacq, J. Phys. Chem. **87**, 2226 (1983).

[9]S. Martin, J. Chevaleyre, M. Chr. Bordas, S. Valignat, and M. Broyer, J. Chem. Phys. **79**, 4132 (1983).

[10]M. J. Seaton, Proc. Phys. Soc., London **88**, 801 (1966).

[11]M. C. Bordas, M. Broyer, P. Labastie, and B. Tribollet, to be published.

[12]C. Greene, U. Fano, and G. Strinati, Phys. Rev. A **19**, 1485 (1979).

[13]K. T. Lu, Phys. Rev. A **4**, 579 (1971).